Landscape Ecology **19:** 401–415, 2004.

Research article

Simulated productivity of heterogeneous patches in Southern African savanna landscapes using a canopy productivity model

Kelly K. Caylor[1,2,*] and Herman H. Shugart[2]
[1]*Department of Civil and Environmental Engineering, Princeton University, Princeton, NJ 08544;*
[2]*Department of Environmental Sciences, University of Virginia, Charlottesville, VA 22904;* [*]*Author for correspondence (e-mail: kcaylor@princeton.edu)*

Received Date 14 March 2003; accepted in revised form 22 September 2003

Key words: Vegetation structure, Vegetation productivity, Africa, Botswana, Kalahari, Spatial heterogeneity

Abstract

A daily model of terrestrial productivity is used to simulate the annual productivity of heterogeneous vegetation structure at three savanna/woodland sites along a large moisture gradient in southern Africa. The horizontal distributions of vegetation structural parameters are derived from the three-dimensional canopy structure generated from detailed field observations of the vegetation at each site. Rainfall and daily climatic data are used to drive the model, resulting in a spatially explicit estimate of vegetation productivity in 100 m^2 patches over an area 810,000 m^2 (8,100 patches per site). Production is resolved into tree and grass components for each subplot. The model simulates the relative contribution of trees and grasses to net primary productivity (NPP) along the rainfall gradient. These simulated production estimates agree with previously published estimates of productivity in southern African savannas. Water-use efficiency of each site is directly related to the structural composition of the site and the differing water-use efficiencies for tree and grass functional types. To assess the role of spatial scale in governing estimates of vegetation productivity in heterogeneous landscapes, spatial aggregation is performed on the canopy mosaic at the northern-most (wettest) site for 625 m^2, 2500 m^2 and 5625 m^2 resolutions. These simulations result in similar overall patterns of average NPP for both trees and grasses, but drastically reduced distributions of productivity due to reduced structural heterogeneity. In particular, the aggregation of the detailed spatial mosaic to coarser resolutions is seen to eliminate information regarding demographic processes such as regeneration and mortality, and the dependence of grass productivity on over-story density. These results indicate that models of system productivity in savanna/woodland ecosystems must retain high spatial resolution to adequately characterize multi-year structural responses and to accurately represent the contribution of grass biomass to overall ecosystem production.

Introduction

The ability to estimate patterns of primary productivity and predict changes in productivity associated with environmental and vegetation change is essential to both resource management and global change science. Logically, realistic representation of vegetation productivity requires detailed representation of physiological processes such as assimilation and transpiration as well as an accurate characterization of the vertical and horizontal components of vegetation structure, such as canopy cover, canopy leaf area, and vegetation biomass (Gholz et al. 1997; Scholes and Vanbreemen 1997; Asner et al. 1998; Dowty et al. 2000). Often modeling exercises focus on simulating detailed processes, but rely on simple representations of vegetation structure that do not take into account spatial heterogeneity in vegetation structural pattern (Shugart 1998). In many cases, this emphasis on 'process' over 'pattern' occurs due to the use of point

observations that are based on assumptions of spatial homogeneity (i.e., flux towers) or spatial aggregation (i.e., remote sensing) that reduces spatial heterogeneity.

Savanna net primary production (NPP) is primarily limited by the magnitude and seasonality of annual rainfall (Walker 1987), and there exists a strong link between carbon uptake through photosynthesis and water loss through transpiration in savanna vegetation (Cook et al. 2002). However, variations in vegetation composition (tree/grass cover) and structure (LAI, biomass) have the potential to greatly alter estimates of both production and transpiration for the same amount of rainfall (Golluscio et al. 1998; Belsky et al. 1993). The ratio of these coupled fluxes of carbon and water is denoted as the water use efficiency (WUE), and values of WUE can be defined (and measured) at a number of spatial and temporal scales from instantaneous leaf-level gas exchange to annual ecosystem rainfall and productivity relationships (Larcher 1995). In general, savanna tree and grass vegetation exhibit characteristically different WUE values due to changes in leaf-level physiology and life history strategies. With respect to physiology, the C_4 photosynthetic pathway used by grasses in many warm-season savannas allows for reduced levels of photorespiration relative to the C_3 pathway used by woody vegetation. The transfer of carboxylation into bundle sheaths during C_4 photosynthesis where oxygen concentration is low increases the carbon yield of C_4 photosynthesis per unit water transpired. In addition to physiological differences, the life history of grasses is such that more biomass is allocated to photosynthetic tissue than woody vegetation. The reduced allocation of grasses to structural tissue further differentiates the water use of trees and grasses when measured at the whole-plant level over annual time frames (Scholes and Walker 1993).

Because of the pronounced physiological and ecological divergence between trees and grasses, tropical water-limited ecosystems are particularly appropriate for ecohydrological analyses which relate tree/grass interactions to soil moisture dynamics and water use (Rodriguez-Iturbe et al. 1999; Porporato et al. 2003). However, savanna ecosystems present a particular challenge regarding the relationship between water use and rates of production, due to the significant functional interactions that occur between trees and grasses at relatively small spatial scales (Scholes and Archer 1997). Trees modify both the light and moisture environment underneath their canopies, with significant consequences on grass production and efficiency. In addition, the high degree of heterogeneity in tree canopy structure and stem biomass further complicates the derivation of simple relationships between water use and production for woody vegetation in semi-arid ecosystems. Given the small spatial scales over which savanna vegetation varies (typically, ~10-100 m) and the demonstrated importance of tree/grass interactions, the effect of spatial aggregation on estimates of tree/grass production and water use efficiency could be significant. For instance, it is quite likely that use of 'average' vegetation structure at larger scales (~500-1000 m) may bias estimates of both productivity and water use efficiency in savanna ecosystems.

The Kalahari region of southern Africa is ideal for studying the relationship between productivity, water use efficiency, and patterns of vegetation structure. The Kalahari Transect (KT) is one of a number of IGBP transects designated throughout the world (Koch et al. 1995), and covers a latitudinal rainfall gradient varying from 250 mm/year in the south to 1000 mm/year in the north. The large gradient in both the mean and variation of annual rainfall results in dramatic changes in vegetation structure across the study sites, which have been extensively characterized (Scholes et al. 2002; Caylor et al. 2003; Privette et al. in press). Vegetation type ranges from partially closed woodlands in the north to open shrubland in the south. Throughout the KT, the mixed tree/grass composition characteristic of savanna communities is maintained. Consistency in geomorphology over the entire region – primarily deep Kalahari sands (Thomas and Shaw 1991) – allows for an analysis of vegetation structure and ecosystem processes independent of soil type.

This study employs a previously developed mechanistic model of water and carbon fluxes that considers the distribution of tree and grass canopies aboveground and rooting patterns belowground (Dowty 1999). An earlier application of the model has shown it to adequately represent the dynamics and magnitude of Kalahari vegetation productivity in response to inter-annual variation in rainfall (Dowty et al. 2000), and additional analysis has shown the potential impact that vegetation canopy structure can have on the range of simulated vegetation production estimates both within and between sites (Caylor et al. in press). Our current effort expands these prior results by explicitly considering the effect of spatial heterogeneity on estimates of NPP and WUE at a se-

ries of sites across the Kalahari rainfall gradient. In addition, we examine the consequences of minimizing spatial heterogeneity in the analysis of system productivity and water use efficiency. Because NPP and transpiration (and therefore WUE) are mass fluxes that imply an underlying temporal and spatial context, it is important to clarify the spatial and temporal extent of our measurements. Throughout this study, we characterize the NPP of both trees and grasses as the sum of simulated daily NPP for a 10 × 10-meter patch of vegetation during the growing season, and we characterize WUE for both trees and grasses as the ratio of the sum of daily NPP during the growing season to the sum of simulated daily transpiration within each 10 × 10-meter patch over the same period. Using these metrics of savanna vegetation performance, we define two separate goals:

Assess the effect of patch scale heterogeneity in vegetation structure on estimates of annual net primary productivity and annual tree/grass water use efficiency.

Examine the effect of spatially aggregating vegetation structure on simulation estimates of primary productivity at the northern-most (wettest) site used in the study.

Methods

Productivity model description

Our model simulates CO_2 uptake by photosynthesis, along with respiration and evapotranspiration on a daily basis. It requires daily rainfall, mean temperature, relative humidity, and average wind speed as data input. It is convenient to divide the model into four components: leaf physiology, canopy processes, soil water balance, and leaf phenology. To a large extent, each of these model components is derived from previously published models. A brief presentation of the modeling approach is presented here. More detailed derivations and explanations are available from Dowty (1999), as well as the citations provided below.

The leaf physiology component includes models for C_3 and C_4 photosynthesis, stomatal conductance and CO_2 and water diffusion through the stomata. All tree leaves are assumed to assimilate CO_2 by the C_3 photosynthetic pathway and all grasses are assumed to assimilate CO_2 by the C_4 pathway. The biochemical model of C_3 photosynthesis is based on the Harley et al. (1992) implementation of the Farquhar et al. (1980) model with only minor modification as presented in Woodward et al. (1995). Leaf level assimilation within the C_3 model proceeds through the establishment of the minimum rate of carboxylation derived from limiting controls on photosynthesis. These rates are based on limitations due to enzyme kinetics and substrate availability. Analogous to the C_3 model, the C_4 model also considers three rate-limiting processes. The major difference between the C_3 and C_4 models is increased substrate regeneration limitation in the C_4 model due to additional enzyme requirements associated with the C_4 pathway, and a generally reduced kinetic limitation in the C_4 model caused by a reduction of oxygenation relative to C_3 photosynthesis (Pearcy and Ehleringer 1984).

Stomatal conductance is calculated with the model of Ball et al. (1987) modified to include a response to soil moisture as in Woodward et al. (1995). The composite empirical relationship between stomatal conductance and environmental conditions is based on the stomatal conductance at the light compensation point for photosynthesis and an empirical sensitivity coefficient. These responses follow the linear formulations presented in Woodward et al. (1995), which are based on observations from a range of climates (Woodward et al. 1994). Soil moisture constrains stomatal conductance according to the function presented in Woodward et al. (1995).

In a hierarchical approach, the leaf model is embedded in a canopy model that considers radiation attenuation through the canopy and allocates nitrogen to both trees and grass. Leaf level irradiance throughout the canopy is based on a Beer's law attenuation of incident abovecanopy irradiance (Shugart 1984). Incoming photosynthetically active radiation (PAR) is derived from total shortwave incoming radiation based on solar geometry and empirical relationships between total incoming and the PAR portion of shortwave radiation (Campbell and Norman 1998). Nitrogen is allocated based on light availability in each layer, and the soil nitrogen content (Woodward et al. 1995), which is assumed to be constant over the year of simulation presented. Leaf boundary layer conductance and transpiration are calculated using isothermal net radiation, via a modified Penman-Monteith equation (Jones 1992). Canopy conductance is derived from the logarithmic wind profile and vegetation canopy height (Campbell and Norman 1998). There is a corresponding vertical root profile for both trees and grass, which have distinct distribu-

tions of root mass through a three-layer soil profile. In each case root mass is a constant fraction of whole-plant mass with a fixed allocation to each soil layer. Canopy respiration is calculated in two parts. Maintenance respiration is a function of temperature and plant mass, while growth respiration is a function of biomass increment. Both of these two approaches follow the presentation in Woodward et al. (1995).

The soil water balance for each of the three soil layers is a simple sum of inputs from rainfall (or drainage from the overlying layer), outputs from plant transpiration (dependent on root mass and available water) and soil evaporation from the top layer only. Bare soil evaporation is determined according to the relationship in Sellers et al. (1996), but is only calculated in plots that do not contain a tree canopy. Soil evaporation is further constrained by the amount of bare soil within each patch. This implementation of soil evaporation is used to eliminate the difficulty in determining the energy budget terms necessary to derive soil temperature under a dynamic tree canopy at daily time steps.

Because the exact nature of the mechanisms promoting leaf flush and leaf fall in the savannas of southern Africa is unknown, leaf phenology is handled using two distinct modeling approaches. The first approach is deterministic in nature and prescribes leaf flush and leaf fall at the onset and end of the wet season respectively. The second method allows the timing and, to a lesser extent, the rate of leaf flush and leaf fall to depend primarily on the intensity and persistence of available soil moisture conditions. All simulations presented here employ the deterministic leaf phenology model, with leaf flush beginning Sept. 1st, the start of the wet season, and leaf fall initiating in late April at the start of the dry season.

Field data collection

At each site, vegetation structure has been extensively characterized through the use of detailed stem mapping and grass biomass sampling (Caylor et al. 2003; Scholes et al. 2002). The three sites used in this study range across a rainfall gradient from the north to south. The northernmost site, Kataba Forest (15.44S, 23.25E), is a Kalahari woodland with characteristic miombo vegetation (*Brachystegia* sp.) and receives an average of 879 mm of rainfall per year. The southernmost site, Tshane (24.17S, 21.89E), receives 365 mm of rainfall per year and is a wooded (*Acacia* sp.) grassland. The intermediate site, Pandamatenga Agricultural Station (18.66S, 25.50E), is a woodland dominated by both *Schinziophyton* and *Baikiaea* species and receives an average of 698 mm of rainfall each year. Detailed site descriptions and methodologies are provided in Scholes et al. (2002) and Caylor et al. (2003). A variable-width belt-transect approach was used for stem mapping. Tree location, species, diameter, height and major and minor axis of crown dimensions were measured for each individual taller than 1.5 meters. For multi-stemmed individuals, the diameter of each stem was recorded separately. Individual locations were determined to be the center of the main stem, or the estimated center when multiple-stemmed individuals were sampled. Canopy area was calculated to be an ellipse defined by two major axes of measurement. Heights to the base and top of each individual canopy were determined using a clinometer. Leaf biomass and whole-tree biomass are estimated for each individual using generalized allometric relationships developed in Goodman (1990) as modified by Dowty et al. (2000). Field measurements of specific leaf area [m^2/kg] were used to calculate total leaf area from each tree's allometrically determined leaf biomass. Grass biomass was determined by harvesting ten to twenty 1 m^2 quadrats at each site. Samples were dried and weighed to determine dry grass biomass per square meter. Plant physiological parameters necessary to implement the productivity model are based on leaf-level gas exchange observations of representative tree and grass species taken during peak growing season conditions (Dowty 1999). At each site the variation in plant physiology is characterized by two sets of parameters – one each for C_3 and C_4 vegetation. Although this method ignores the species-specific variation present in physiological parameters, it serves to capture the main differences that exist between tree and grass leaf-level physiology within the study sites.

Canopy structure parameterization

To assess the effect of spatial heterogeneity on model estimates of vegetation productivity, the relationships derived from the detailed stem map data are used to generate a simulated 900m × 900m vegetation mosaic. The mosaic is created by randomly distributing individual trees with structural properties (diameter, height, canopy dimension, biomass and leaf area) sampled from the actual distribution of trees observed in the field. The combination of canopy dimension

and individual height produces a three-dimensional representation of canopy structure throughout the 900m × 900m landscape at a resolution of 1 meter. A toroidal edge-correction technique is employed to remove bias associated with plot boundaries. Leaf area per unit canopy volume is determined by distributing total leaf area for each individual evenly throughout each individual's canopy volume.

Canopy volumetric distribution is modeled in 1-meter increments vertically and horizontally using the observed axis of canopy width (a_1 and b_1) as well as the individual's observed height (h_1), where a_1, b_1 and h_1 are all in meters. The base of each individual's canopy (h_b) is determined from field observations or is set to $1/3h_1$ when no observation of canopy base height is available. For vegetation with heights of 2 meters or less, canopy base is taken to be the ground. The total depth of the canopy (h_c), and the midpoint of each canopy (h_m) are found as $h_c = h_1 - h_b$ and $h_b + h_c / 2$ respectively. At each layer d in the canopy ($d = h_1$ to h_b), canopy width in each axis is modeled as

$$a_d = \sqrt{a_1^2\left(1 - \frac{(d-h_m)^2}{(h_1-h_m)^2}\right)} \qquad if \quad d - h_m > 0$$
$$b_d = \sqrt{b_1^2\left(1 - \frac{(d-h_m)^2}{(h_1-h_m)^2}\right)}$$

$$a_d = a_1 \exp\left(4\,\frac{d-h_m}{h_m}\right) \qquad if \quad d - h_m < 0$$
$$b_d = b_1 \exp\left(4\,\frac{d-h_m}{h_m}\right)$$

This method provides an idealized canopy geometry that closely mimics the shape of a typical savanna tree crown. Volume is summed over the canopy, and each individual's leaf area is distributed evenly throughout the individual's canopy volume, to arrive at a leaf area per unit volume, or leaf area density [m^2/m^3]. Where canopy volumes intersect, leaf area density at intersecting locations is taken to be the sum of the contributing canopies' leaf area densities. Total stem biomass is assumed to be contained entirely within the 1 × 1 m^2 cell containing the location of each individual. The result is a 900 × 900 meter mosaic of vegetation structure resolved at 1-meter increments in all three dimensions. This grid of vegetation structure is then sub-sampled into 10 × 10m patches for use in the physiological model, resulting in 8,100 patches per site. Leaf area is determined by taking the average of the total leaf density through the canopy profile at each 1-m^2 grid location within the 100-m^2 subplots. This method of spatial averaging removes information on the vertical profile of the woody canopy (i.e., the canopy is represented as a single 'big leaf'), while maintaining information regarding the small-scale horizontal variation in canopy height, leaf area, and stem biomass. In the case of the Kataba site, the 1-meter grid is also sub sampled at 25- 50- and 75-meter resolutions.

We tested the degree that the simulated vegetation canopy structure represents the true distribution of canopy vegetation at the sites by estimating the distribution of below-canopy shortwave radiation for the simulated structure of the Kataba Forest site and an actual transect of below-canopy observations of shortwave incoming radiation (SW_{BC}) taken during March 2000 (Privette et al. 2002) at the same site (Figure 1). The highest value of observed SW_{BC} is the above-canopy value (SW_{INC}). The distribution of SW_{BC} for the simulated structure is then determined at 1-meter increments using Beer's law ($SW_{BC} = SW_{INC}\ e^{-k}\ LAI_c$) and the canopy leaf area index (LAI_C). The resulting cumulative distribution of SW_{BC} derived from the simulated structure is compared to the observed SW_{BC}. The two distributions are in substantial agreement except at high levels of SW_{BC} (i.e., low LAI_C). The fit is sufficient to provide some confidence in the simulated structure's representation of canopy vegetation structural heterogeneity.

Climate/meteorological data

The productivity model used in this study requires a suite of daily meteorological data including average daily temperature, daily mean relative humidity and rainfall. These data are often unavailable for many locations in the Kalahari, and the use of distant station data is problematic due to the highly convective and patchy nature of rainfall in the Kalahari region. Therefore, simulations of annual productivity are conducted using daily climate data based on a combination of both stochastic and empirical modeling techniques.

The daily productivity model requires mean daily data of temperature, relative humidity and wind speed. At all sites, wind speed is assumed to be constant at 1 m/s. For this study, stochastic variation in temperature and relative humidity are ignored, and an

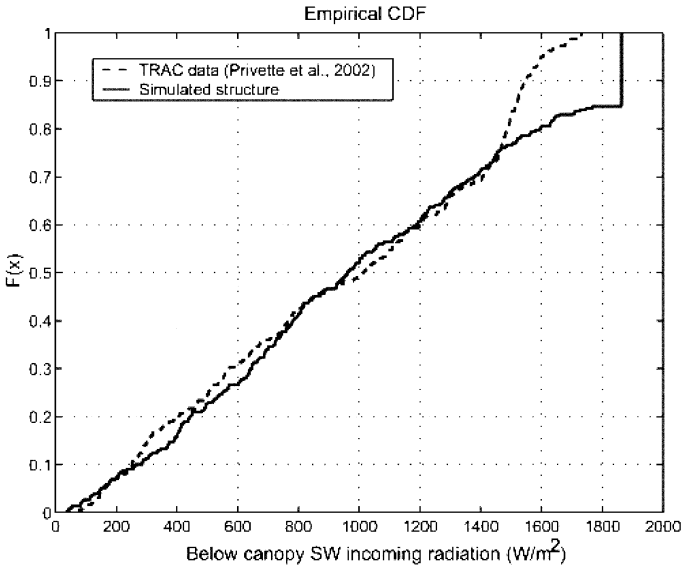

Figure 1. Comparison of the cumulative distributions for both estimated SW_{BC} radiation under the 'simulated' vegetation structure (solid line) and observed SW_{BC} radiation under the tree canopy measured at the Kataba forest site (dashed line – (Privette et al. 2002)). Estimated SW_{BC} below the simulated vegetation structure was determined using Beer's law and a shortwave extinction coefficient of 0.35. Both data sets are sampled at 1-meter frequency to capture the small-scale changes in vegetation canopy structure. The two distributions are in very high agreement for most values of incoming radiation, and diverge at when incoming radiation is greater than 1450 W/m^2. This range of radiation corresponds to tree canopy LAI values less than 1.0, and is likely due to the fact that the observed data samples some degree of below-canopy shrub and herbaceous vegetation, which is not included in the simulated vegetation structure.

Table 1. Correlation coefficients between observed and predicted values of mean daily temperature and mean daily humidity. Reduced model predictive power at Vastrap is a result of highly variable observed daily humidity data.

Site	Lattitude	Longitude	Model Correlation Coefficient C(obs,model)	
			Daily Mean Temperature	Daily Mean Humidity
Kataba Forest Reserve Mongu, Zambia	15.44 S	23.25E	0.97	0.96
Sachinga Agricultural Station Katima Mulilo, Namibia	17.70 S	24.08 E	0.95	0.86
Sandveld Research Station Gobabis, Namibia	22.02 S	19.17 E	0.95	0.70
Vastrap Weapons Range Upington, South Africa	24.17 S	21.89 E	0.91	0.30

empirically derived 5th-degree polynomial approximation of daily temperature and humidity is used. The daily climatology of mean temperature and humidity are derived from a series of relationships based on daily temperature and humidity records at 4 stations along the Kalahari Transect (Table 1). At each station, a 5th-degree polynomial is fit between the day of year (t_D, Sept 1st – October 31st) and the 2-year average of daily mean temperature ($\overline{T}_a$) and humidity ($\overline{q}$). The polynomial parameters describing the station data each of the four sties are found to vary with annual rainfall between stations and these patterns are used to estimate polynomial parameters and subsequent daily meteorological data at locations where only mean annual rainfall is known. For any given mean annual rainfall, polynomial parameters are estimated using an inverse weighting method between the two rainfalls that bound the mean annual rainfalls of interest. The stations used in model development are representative of a wide range of mean annual precipitation across (879-216 mm) and polynomial parameters for most mean annual precipitation values can be estimated in this manner. Unlike the empirical method used for temperature and relative humidity, rainfall is modeled stochastically using the probabilistic rainfall delivery method developed by Laio et

al. (2001) with parameters inferred from Porporato et al. (2003). Although daily rainfall is modeled as a purely stochastic process, the simulated yearly pattern used is constrained to be within 5% of the long-term mean annual rainfall at each site.

Model simulations

For each site, a yearly simulation of daily productivity was conducted for each of the 8,100 10 × 10 meter patches. Annual sums of daily tree and grass NPP (NPP_{TREE} and NPP_{GRASS}, respectively) at each patch were then used to investigate the heterogeneity in simulated productivity. In addition, the annual water use efficiency of trees and grasses (WUE_{TREE} and WUE_{GRASS}, respectively) in each patch is determined using the ratio of total annual NPP (g-C) and total water transpired (mm-H_2O). Total landscape water use efficiency at each site is the simple average of annual water use efficiency in each of the 8,100 patches. In addition to simulations of 10 × 10 meter patches, additional simulations of aggregated 25 × 25m, 50 × 50m and 75 × 75 meter patches are conducted at the Kataba forest site. The distribution of tree and grass productivity and water use efficiency at each of these spatial scales is investigated.

Results

Productivity of 10 × 10 meter patches

Average tree productivity simulated for the 8,100 patches at each site decreases along the rainfall gradient, with an average annual tree productivity of 1131.6 g-C/m^2 at Kataba Forest, 678.5 g-C/m^2 at Pandamatenga and 11.2 g-C/m^2 at Tshane (Figure 2a, Table 2). Simulated annual grass productivity is also variable across the gradient, with average productivity of 255 g-C/m^2 at Kataba Forest, 602.2 g-C/m^2 at Pandamatenga and 596.1 g-C/m^2 at Tshane. Taken together, the total average productivity of each site is 13.9 ton-C ha^{-1} at Kataba Forest, 12.8 ton ha^{-1} at Pandamatenga and 7.1 ton-C ha^{-1} at Tshane. These amounts of annual NPP are in the range of reported NPP estimates of African savannas provided in Scholes and Hall (1996). At all sites, spatial variability in productivity is high. The coefficient of variability, the ratio of standard deviation to average, of trees increases from 0.20 at Kataba Forest to 0.35 at Pandamatenga, to a maximum of 0.65 at Tshane. The coefficient of variability for grasses is uniformly high, and ranges from 1.07 at Kataba Forest to 0.63 at Pandamatenga and 0.72 at Tshane.

Water-use efficiency of trees decreases with decreasing rainfall, while the average water use efficiency of grasses is seen to increase in the southern, drier sites (Figure 2b, Table 2). The average water use efficiency increases with decreasing rainfall, with a mean WUE of 1.85 g-C/mm-H_2O at Kataba Forest, 2.25 g-C/mm-H_2O at Pandamatenga, and 2.44 g-C/mm-H_2O at Tshane. The coefficient of variability in annual WUE is relatively uniform − 0.27 at Kataba Forest, 0.33 at Pandamatenga, and 0.35 at Tshane. Figure 3 depicts the changing patterns of tree and grass water use efficiency as a function of tree leaf area at each of the three sites. At all three sites grass water use efficiency is seen to depend on tree LAI, with thresholds of positive grass WUE decreasing from wet to dry conditions across the transect. Tree water use efficiency exhibits greatest variability at the driest site (Tshane, Figure 3c), but scatter in the relationship between tree LAI and WUE is observed at all sites.

Spatial aggregation and productivity simulation

The range of variability in simulated productivity decreases rapidly with increasing spatial scale of structural parameterization (Figure 4, Table 3). Grass productivity is seen to be strongly dependent on tree LAI in the 10 × 10 meter patch simulations, with high grass productivity at low values of tree LAI. Tree productivity exhibits a non-linear response to LAI, with lower tree production predicted at extreme maximum and minimum tree LAI values. Average productivity for trees at Kataba increases with greater levels of spatial aggregation, while estimates of grass productivity decrease at larger spatial scales (Table 3). Variability in productivity decreases for both trees and grasses, although the reduction in variability of tree productivity is much greater than the reduction in variability of grass productivity. In addition, at spatial scales greater than 10 × 10 meters, the strong dependence of tree and grass productivity on tree leaf area index is eliminated, due to the rapid homogenization of vegetation structure at larger spatial scales.

Figure 5 presents woody NPP in each simulated patch as a function of patch biomass and LAI at each of the spatial scales simulated at the Kataba site. At the highest resolution, a pattern of tradeoffs is demonstrated between increasing assimilation associated

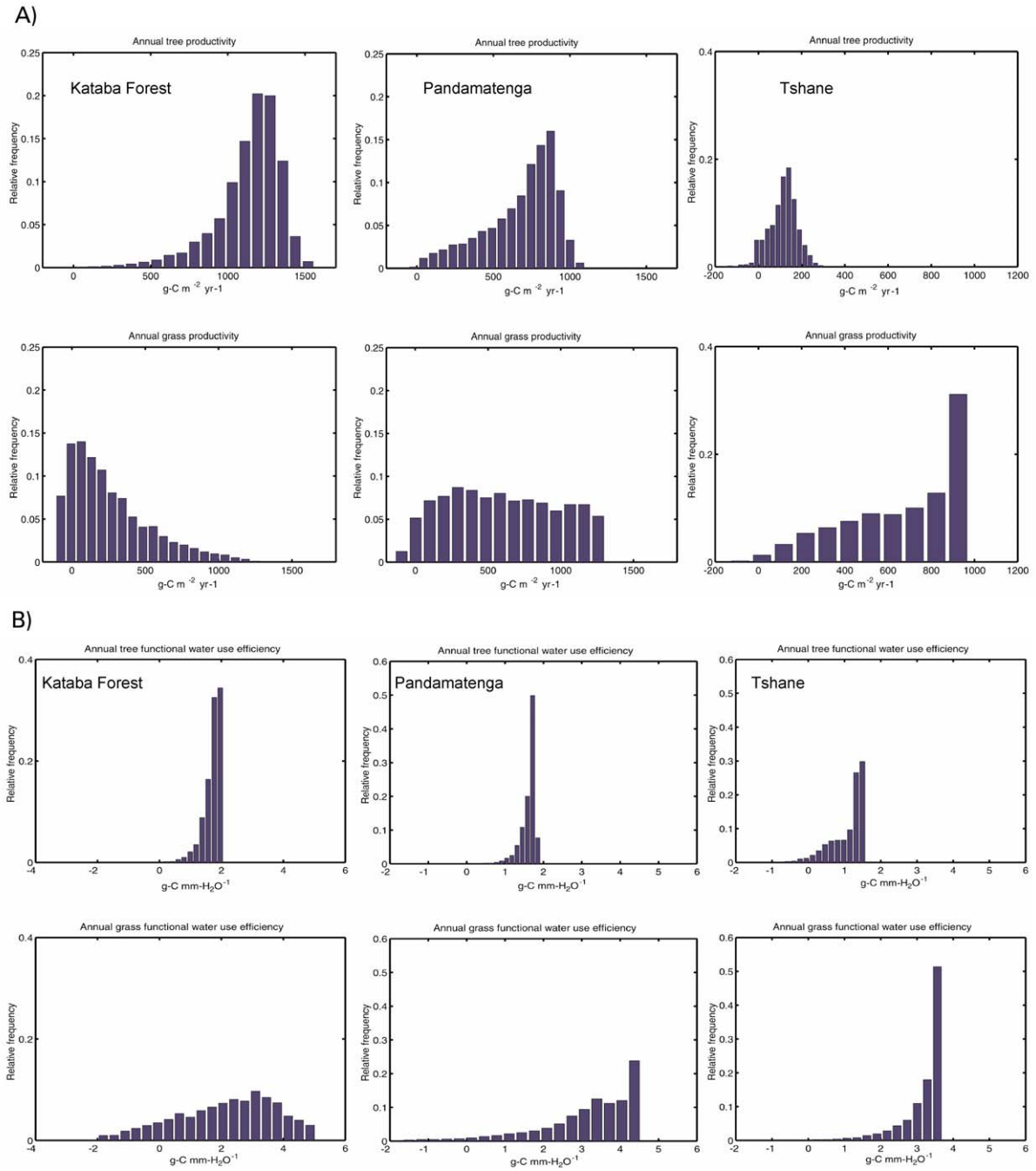

Figure 2. (a) Patch-scale distribution of net primary productivity and water-use efficiency for tree and grass vegetation at the three study sites. The distribution of tree NPP varies with decreasing rainfall across the transect, while the distribution of grass NPP responds to decreasing tree NPP. Simulated NPP below zero indicates insufficient gross productivity relative to respiration associated with standing biomass. (b) Patch-scale distribution of annual water use efficiencies for tree and grass vegetation at the three study sites. Tree water use efficiency is found to be ~0-2 g-C/mm-H_2 O across all three sites, with grass WUE ranging between 0-5 g-C/mm-H_2O. WUE increases for grasses at the more arid site, while tree WUE decreases along the rainfall gradient.

Table 2. Mean annual precipitation (MAP), mean (μ) and standard deviations (σ) of woody leaf area index (LAI), simulated net primary productivity (NPP), and annual water use efficiency (WUE) for trees and grasses across the three study sites. Mean tree production declines with decreasing rainfall, while mean grass production increases. Water use efficiencies of trees and grasses show consistent differences, with grass WUE higher at all sites, and highest at Pandamatenga. Tree WUE decreases with decreasing rainfall. Site-scale WUE increases with decreasing rainfall due largely to the differences in the relative contribution of tree and grass at each site.

Site	MAP (mm)	Tree LAI (m^2 m^{-2})		Tree NPP (g-C m^{-2} yr^{-1})		Grass NPP (g-C m^{-2} yr^{-1})		Tree WUE (g-C mm-H_2O^{-1})		Grass WUE (g-C mm-H_2O^{-1})		Site WUE (g-C mm-H_2O^{-1})	
		μ	σ	μ	σ	μ	σ	μ	σ	μ	σ	μ	σ
Kataba Forest	879	2.46	1.22	1131.6	227.9	255.0	271.6	1.71	0.30	1.93	1.91	1.85	0.50
Pandamatenga	698	1.25	0.89	678.5	235.1	602.2	380.4	1.61	0.21	3.17	1.34	2.25	0.74
Tshane	365	0.62	0.63	111.2	72.2	596.1	428.9	1.09	0.48	2.90	1.56	2.44	0.85

with higher LAI and increased respiration associated with greater standing biomass. The lower edge of the surface in Figure 5a represents patches with the lowest LAI for a given biomass and is typical of patches that contain a single large tree. The upper edge of the response surface represents patches with the maximum LAI for a given biomass, and generally corresponds to a patch with many smaller individuals. Highest woody production is simulated in patches with intermediate LAI and low biomass. At greater spatial scales (Figure 5b-d), these tradeoffs in structure associated with demographics and individual allometry are eliminated.

Discussion

Our first goal in this study was to assess the effect of patch scale heterogeneity in vegetation structure on estimates of annual productivity and annual tree/grass water use efficiency. As expected and discussed above, the rainfall gradient between sites produced significant differences in the average annual productivity of simulated patches between sites. Within sites, the high coefficient of variability in woody leaf area led to even higher coefficients of variability in woody production. At all sites, grass productivity was strongly related to woody LAI, with maximum production in patches with low tree LAI (Figure 2). Tree structure has a strong effect on grass productivity at the Kataba Forest site. Among sites, grass productivity is seen to increase with reduced tree production. The high degree of correlation between grass productivity and tree leaf area reinforces the findings that large tree canopies play an important role in governing the critical distributions of light and moisture availability in Kalahari savannas (Belsky, 1994). In contrast to the concept of direct competition for homogeneously distributed resources, it is likely that the direct control of resource heterogeneity by vegetation structure plays a large role in maintaining the functional diversity in Kalahari savannas. The findings of this modeling exercise are therefore in agreement with field studies of southern African savanna structure which demonstrate the effects of savanna tree canopies on grass production (Dye and Spear 1982), regeneration (Smith and Goodman 1986), spatial pattern (Caylor et al. 2003; Jeltsch et al. 1996; Skarpe 1991) and structural dynamics (Jeltsch et al. 1998).

The water use efficiency of trees is lower than grasses at all three sites (Table 2). Because WUE is calculated at annual scales and based on net production, the differences between trees and grasses are driven by both the increase in leaf-level water use efficiency of C4 (grasses) versus the C3 (tree) photosynthetic pathways, and the decrease in respiration associated with lower structural biomass for grasses relative to trees. As a result of the changing tree/grass composition, site-level water use efficiency increases from north to south, in agreement with the pattern of increasing water use efficiency described observed in eddy flux data by Scanlon and Albertson (in press). The spatially averaged landscape water use efficiency that is observed at a point (as in eddy flux data) can then be seen as the composite of the different water use efficiencies represented by trees and grasses, weighted by their contribution to the overall landscape pattern. In savanna systems, the fluxes of carbon and water from the land surface to the atmosphere are likely to be governed by the distribution and activity of the vegetation. Therefore, the possibility of inverse analysis of the eddy data using footprint analysis to determine the component water use efficiency and productivity of each portion of the

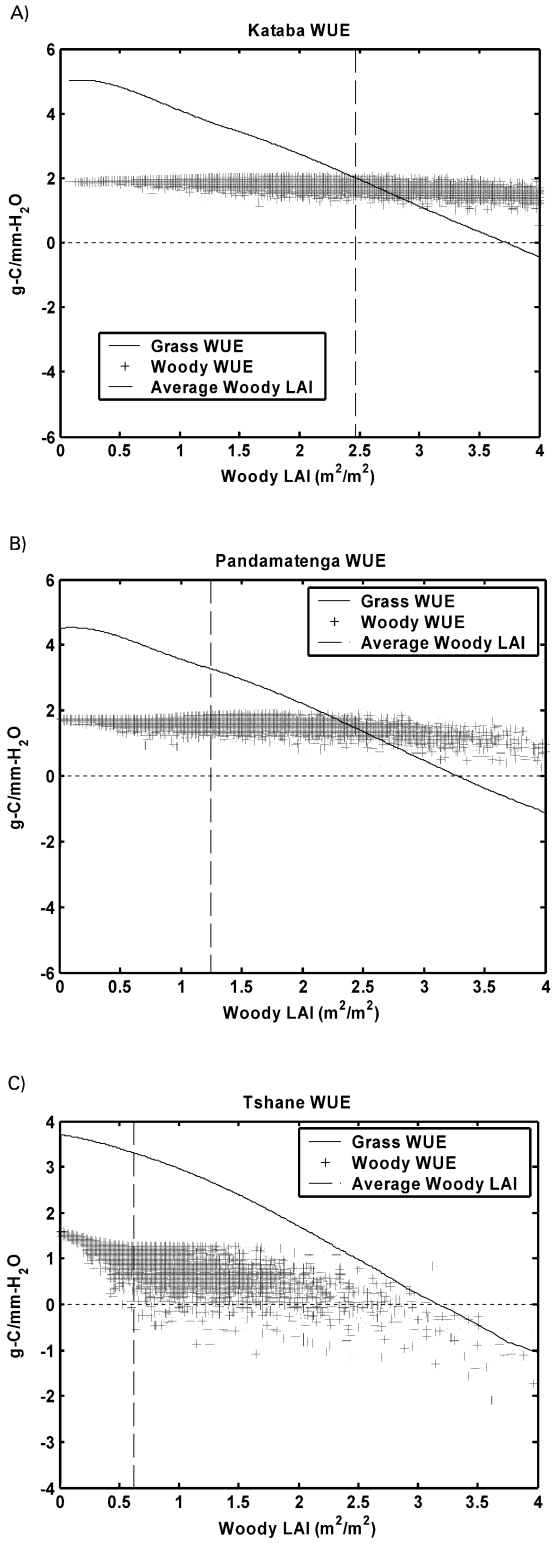

Figure 3. Relationship between woody vegetation LAI and simulated water use efficiency of the woody vegetation canopy (+) and grass understory (-) at the Kataba (a), Pandamatenga (b), and Tshane (c) sites for an average rainfall year. Dashed vertical lines represent average woody LAI at each site. Across all three sites, grass WUE declines with reduced light availability (increased woody LAI), and thresholds of positive grass WUE occur at LAI values of 3.2, 3.4 and 3.7 m^2/m^2 at Tshane, Pandamatenga, and Kataba respectively. Allometric relationships between leaf area, stem diameter and biomass cause scatter in woody WUE as a function of LAI, with the greatest variation occurring at the Tshane site (c.f. Figure 2a). At the Tshane site, 7.3% of the woody vegetation patches exhibit WUE values less than zero.

landscape (trees and grasses) is then possible using the canopy-scale output from a model such as the one provided here.

Across the three sites, tree water use efficiency is typically more uniform than grass water use efficiency (Figure 3). During the wet season, it is likely that grass productivity can be limited by light in many cases under large tree canopies (Ludwig et al. 2001). Trade offs between light and water limitations lead to wide ranges of grass water use efficiency (Figure 2), as similar rates of transpiration lead to varying carbon fixation under diverse light environments. The relationships observed between woody leaf area and grass water use efficiency (Figure 3) demonstrate the importance of the light environment on understory vegetation efficiency in savannas and woodlands. The photosynthesis model tracks light levels below the tree canopy, but does not follow the energy balance of grass and tree canopies explicitly. Transpiration is driven by the atmospheric vapor pressure deficit as modified by stomatal conductance, which is itself constrained by soil moisture. This is accomplished by coupling the modified model of stomatal control, which includes a soil moisture term, to the Penman-Monteith transpiration equation through the shared stomatal resistance term. Typically, the Penman-Montieth formulation considers net radiation, but the current model considerers a formulation that is based on isothermal net radiation, which is a function of atmospheric temperature. Therefore, the rate of transpiration in grasses under tree canopies is largely independent of the energy constraints placed upon the leaf surfaces, as both the vapor pressure deficit and temperature used in the model are average daily observations, and do not vary under tree canopies. A better approximation of the stomatal resistance for grasses shaded by a tree canopy would be an energetic approach that related water loss and carbon uptake to the direct thermal forcing of the leaf, scaled

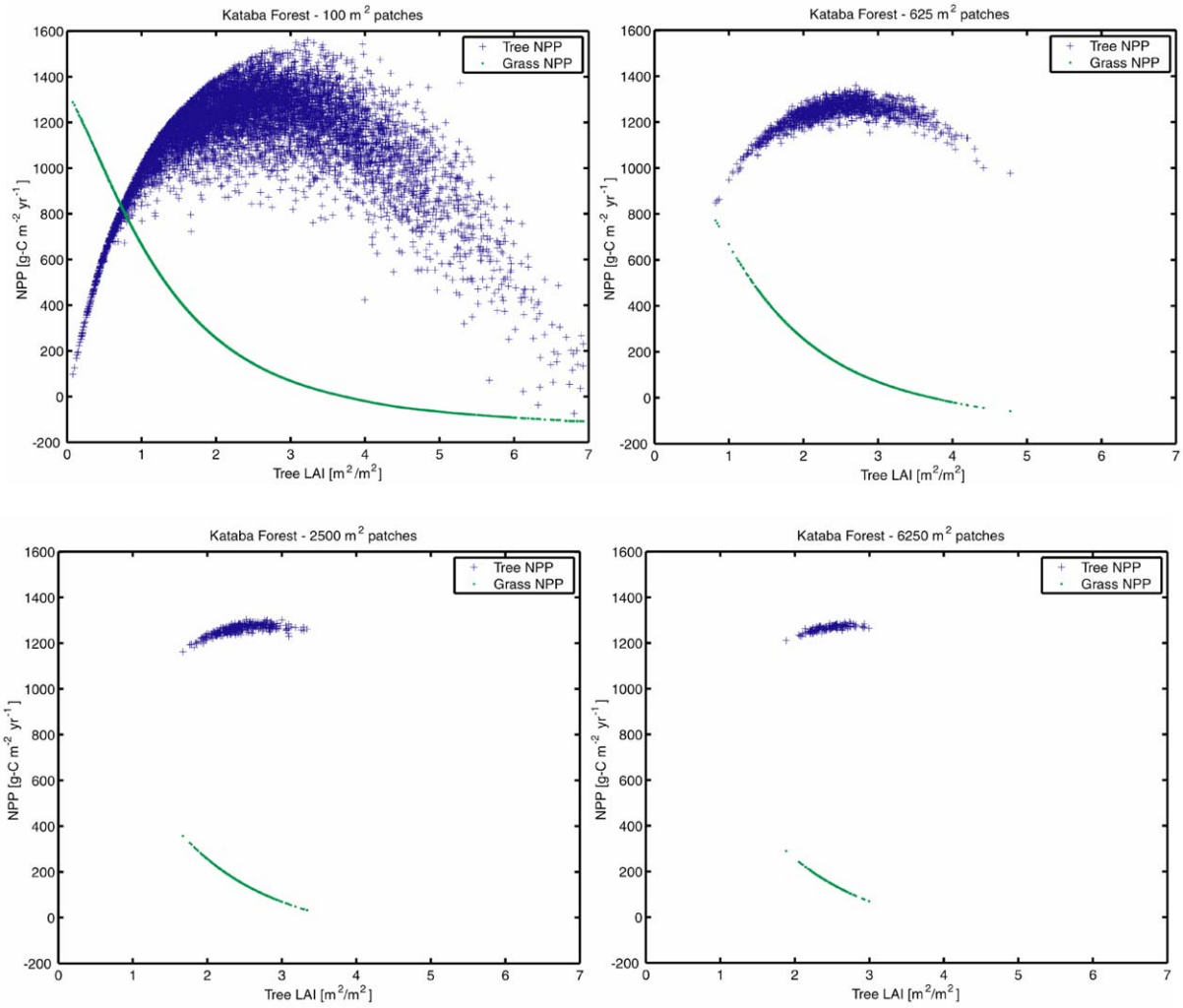

Figure 4. Distribution of tree and grass NPP at 4 different scales of aggregation − 100 m^2, 625 m^2, 2500 m^2 and 6250 m^2 at the Kataba site (Wettest and northernmost site). Increases in the size of patch used for structural parameterization lead to rapid reductions in the range and variability of both tree and grass productivity. In addition, areas of low tree productivity are eliminated, as are areas of high grass productivity. These extremes in productivity are likely related to demographic processes such as regeneration and mortality.

Table 3. Effect of spatial resolution on mean (μ) and standard deviations (σ) of simulated production of trees and grasses at the Kataba site. As the patch size increases, the contribution of grass productivity is reduced, and the estimate of tree productivity increases. Variance in estimates of both tree and grass productivity decrease rapidly with increasing spatial scales.

Resolution (m)	Patch size (m^2)	Tree NPP (g-C m^{-2} yr^{-1})		Grass NPP (g-C m^{-2} yr^{-1})	
		μ	σ	μ	σ
10	100	1131.6	227.9	255	271.6
25	625	1238.4	58.9	177.3	121.3
50	2500	1260.9	21.3	158.3	58.8
75	6250	1265.4	13.2	154.6	40

by soil moisture availability. Under the current implementation, when transpiration is determined after biophysical limitations on assimilation have been determined, it is possible to overestimate water use by shaded vegetation.

Numerous studies have shown that light use efficiency of vegetation is rather constant (Haxeltine and Prentice 1996; Medlyn 1998) but model implementations typically relate light use efficiency to soil moisture status (Prince 1991; Prince and Goward 1995; Hély et al., in press). The findings of this study are that water use efficiency seems to be rather uniform across sites and within vegetation types, but is

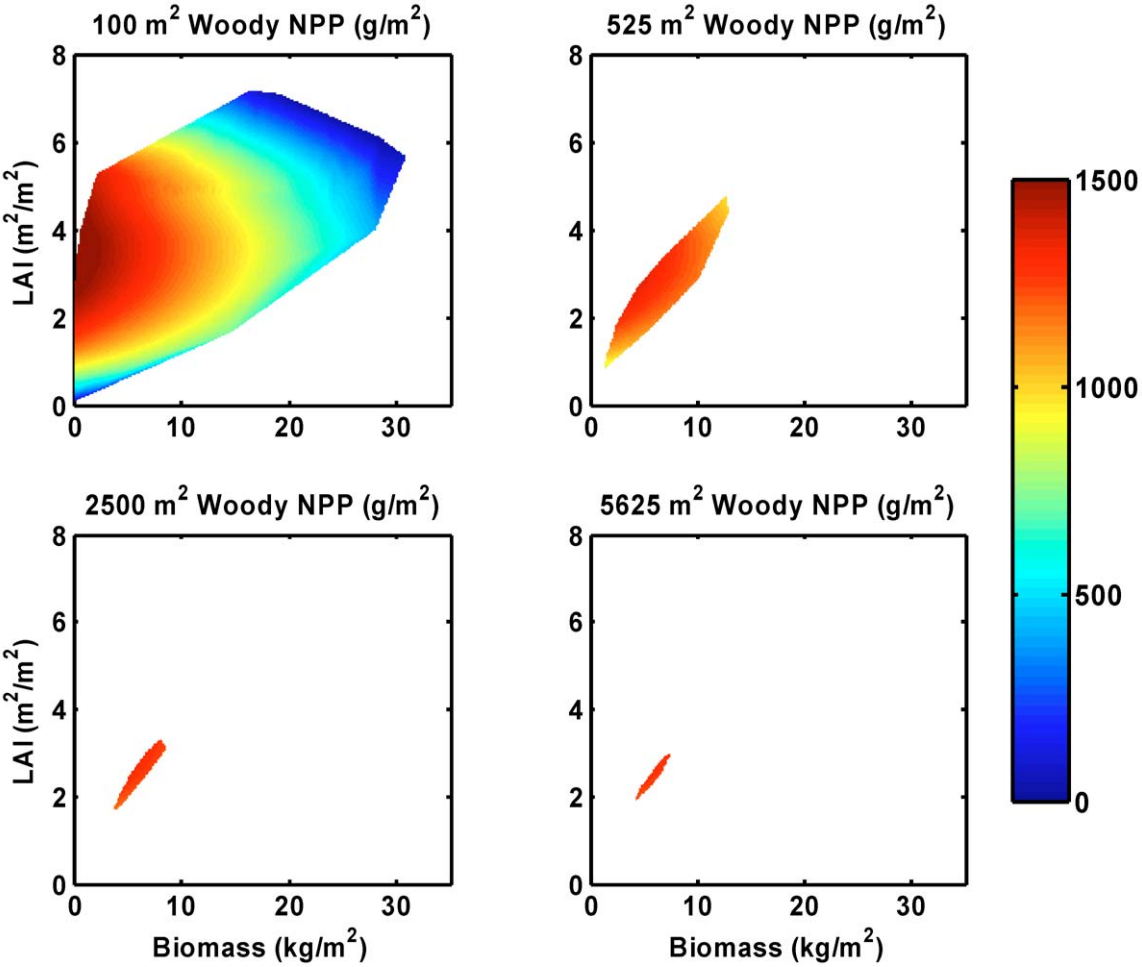

Figure 5. Response surfaces of woody NPP to variation in woody LAI and woody biomass for each of the 4 spatial scales of resolution at the Kataba site. For a given LAI, increases in biomass decrease NPP due to increased respiration. Maximum productivity is observed for intermediate LAI values (~3 m^2/m^2) with low biomass. The consideration of variation in woody biomass explains the scatter in both woody WUE (Figure 3) and woody NPP (Figure 4). Individual allometric tradeoffs between LAI and biomass lead to patch-level constraints on the possible combinations of LAI and biomass with important consequences on estimation of NPP. When considering larger spatial scales, these allometric effects are 'averaged' out of the structural data and the contribution of biomass to the determination of NPP is reduced.

coupled to plant light status in situations where light is limiting (e.g., under tree canopies). These modeling results are in agreement with recent field work on water use efficiency in savanna vegetation (Smit and Rethman 2000). The synthesis of these two concepts raises the interesting possibility that estimates of productivity for trees and grasses in Kalahari savannas could be derived based on the minimum of the light and water use efficiency for each vegetation type based on the combined energy/water constraints.

The scatter in water use efficiency of woody vegetation demonstrated at each of the sites (Figure 3) highlights the importance of structural allometry in determining overall production at the canopy scale. For a given canopy LAI, the underlying individual structure may consist of many small trees or a single large tree. The differences in LAI per unit biomass that arise from varying structural composition at the individual level lead to significant variation in the patch-scale canopy WUE of woody vegetation. We note that tree water use efficiency was most sensitive to LAI/biomass relationships at the southernmost site (Figure 3c), where over 7% of the woody vegetation exhibited negative average WUE over the growing season. These findings reflect the greater sensitivity of woody vegetation to hydrological balance in the drier end of the rainfall gradient, and the need for large trees in southern portions of the Kalahari

Transect to survive periods of low (or even average) rainfall by maximizing production in high rainfall years. Even in the wettest site, the varying LAI/biomass composition of woody vegetation at small spatial scales led to significant scatter in production as a function of leaf area index (Figure 4a).

Our second goal was to examine the effect of spatial aggregation of the spatial mosaic on simulated estimates of primary productivity. This was done at the northern-most and wettest end of the transect. At the highest spatial resolution, tree canopy productivity first increases with increasing leaf area and then decreases, returning to zero at the highest values of woody LAI (Figure 4a). In contrast, the grass component of the vegetation exhibits an exponential decline in NPP with increasing woody LAI. While the pattern in grass NPP is a result of increased light reduction under increasingly higher tree canopy LAI values, the pattern in woody NPP reflects the changing tradeoffs between assimilation, which is a function of leaf area, and respiration, which is a function of standing biomass. For a given woody vegetation canopy, any increase in LAI implies an increase in non-assimilating structural biomass to support the additional leaf area. Our results suggest that for canopy LAI values greater than ~3.5, increases in standing biomass associated with increased LAI generally cause a reduction in overall woody NPP.

There is a rapid reduction in structural variability associated with increased scales of aggregation. As a consequence of reduced structural heterogeneity, the mean and range of variability of the productivity of both trees and grasses changes with the resolution of the data (Table 3). In particular, as the pattern mosaic of vegetation structure is averaged at successively larger spatial scales, the tails of the functional distribution are removed and the average responses are emphasized (Figure 4). At coarser spatial resolutions, the non-linear aspect of tree canopy LAI on light availability is reduced because the presence of tree gaps (patches with low woody LAI) is eliminated. This leads to the exclusion of high productivity grass patches, and an overall reduction in the contribution of grasses to overall NPP at coarser resolutions. In contrast, the average woody NPP increases in patches with coarser spatial resolution (Table 3, Figure 5). Because extremely low LAI values and extremely high biomass values only occur at the smallest spatial scales (10×10 meters), the overall average productivity of the tree canopy increases as the spatial mosaic becomes coarser (Figure 5b-d, Table 3). To some degree, the shape and nature of the response surfaces presented in Figure 5 are a result of the allometric relationships used to derive leaf mass and standing biomass from stem diameters. However, that these allometric relationships yield reasonable distributions of leaf area sufficient to mimic observed below-canopy light availability (Figure 1) lends some support to their utility.

The accurate characterization of multi-year vegetation structural dynamics requires sufficient information on vegetation function to apply the stochastic components of mortality and regeneration to vegetation pattern. When spatial pattern is averaged over successively larger spatial scales it becomes very difficult to assess how environmental variability will lead to structural changes, since the central tendency of the spatial mosaic will not respond with the same dynamics as the extremes of vegetation structure. Using a simulation model that resolves the productivity of vegetation structure at a relatively fine scale, we have demonstrated that vegetation processes applied to this structure at different resolutions produce changes in such fundamental indices of vegetation performance as water-use efficiency and productivity. This can be demonstrated in much more abstract terms because non-linear models, such as those used to represent plant water and CO_2 fluxes, are not superposable and there are attendant difficulties in upscaling underlying model parameters derived from vegetation structure at different scales. That the result can be found in a realistic vegetation model with reasonable parameter estimates for actual plant canopies is more significant in indicating this effect could occur for real vegetation at real resolutions. Certainly these results speak for at caution (at least) in relating modeled productivity at one scale to data on productivity collected at another scale. There are similar implications for interpretation or modeling plant processes at larger spatial scales using laboratory or fine-scale estimates of fundamental processes.

References

Asner G.P., Bateson C.A. and Wessman C.A. 1998. Estimating vegetation structural effects on carbon uptake using satellite data fusion and inverse modeling. Journal of Geophysical Research 103: 28–39.

Ball J.T., Woodrow I.E., and Berry. J.A. 1987. A Model Predicting Stomata Conductance and its Contribution to the Control of Photosynthesis Under Different Environmental Conditions. In:

Biggens J. (ed.), Progress in Photosynthesis Research, Vol. IV. Martinus Nijhoff Publishers, Dordrecht, The Netherlands.

Belsky A.J., Mwonga S.M., Amundson R.G., Duxbury J.M. and Ali A.R. 1993. Comparative effects of isolated trees on their undercanopy environments in high and low-rainfall savannas. *Journal of Applied Ecology* 30(1): 143–155.

Belsky A.J. 1994. Influences of trees on savanna productivity: Tests of shade, nutrients and tree-grass competition. Ecology 75: 922–932.

Campbell G.S. and Norman J.M. 1998. An Introduction to Environmental Biophysics, 2nd edition. Springer-Verlag, New York, New York, USA.

Caylor K., Shugart H. and Smith T.M. 2003. Tree spacing along the Kalahari Transect. Journal of Arid Environments 54(2): 281–296.

Caylor K.K., Dowty P.R., Shugart H.H. and Ringrose S. in press. Vertical patterns of vegetation structure along the Kalahari Transect: The importance of spatial heterogeneity in modeling system productivity. Global Change Biology.

Cook G.D., Williams R., Hutley L.B., O'Grady A. and Liedloff A. 2002. Variation in vegetation water use in the savannas of the North Australian Tropcial Transect. *Journal of Vegetation* Science 13(3): 413–418.

Dowty P., Caylor K.K., Shugart H.. and Emanuel W.R. 2000. Approaches for the estimation of primary productivity and vegetation structure in the Kalahari region. In: Ringrose S. and Chanda R. (eds), Towards Sustainable Natural Resource Management in the Kalahari Region. University of Botswana, Gaborone, Botswana.

Dowty P.R. 1999. Modeling Biophysical Processes in the Savannas of Southern Africa. PhD. University of Virginia, Charlottesville, Virginia, USA.

Dye P.J. and Spear T. 1982. The Effects of Bush Clearing and Rainfall Variability on Grass Yield and Composition in South-West Zimbabwe. Zimbabwe Journal of Agricultural Research 20: 103–118.

Farquhar G.D., von Caemmerer S. and Berry J.A. 1980. A Biochemical Model of Photosynthetic CO2 Assimilation in Leaves of C3 Species. Planta 149: 78–90.

Gholz H.L., Nakane K. and Shimoda H. 1997. The use of remote sensing in the modeling of forest productivity. Kluwer Academic Publishers, Dordrecht; Boston.

Golluscio R.A., Sala C.E. and Lauenroth W.K. 1998. Differential use of large summer rainfall events by shrubs and grasses: a manipulative experiment in the Patagonian steppe. Oecologia 115: 17.

Goodman P.S. 1990. Soil, Vegetation and Large Hebivore Relations in Mkuzi Game Reserve, Natal. PhD. University of the Witwatersrand.

Harley P.C., Thomas R.B., Reynolds J.F. and Strain B.R. 1992. Modelling photosynthesis of cotton grown in elevated CO2. Plant, Cell and Environment 15: 271–282.

Haxeltine A. and Prentice I.C. 1996. A general model for the light-use efficiency of primary production. Functional Ecology 10: 551–561.

Hély C., Caylor K.K., Dowty P.R., Alleaume S., Korontzi S., Korontzi S., Swap R.J., Shugart H.H. and Justice C.O. in review. A temporal and spatially explicit fuel load model for savannas in southern Africa. Journal of Ecological Modelling.

Jeltsch F., Milton S., Dean W.R.J. and v. Rooyen N. 1996. Tree spacing and coexistence in semiarid savannas. Journal of Ecology 84: 583–595.

Jeltsch F., Milton S.J. and Moloney K.A. 1998. Modelling the impact of small-scale heterogeneities on tree-grass coexistence in semi-arid savannas. Journal of Ecology 86: 780.

Jones H.G. 1992. Plants and microclimate: a quantitative approach to environmental plant physiology. Cambridge University Press, Cambridge, New York, USA.

Koch G.W., Vitousek P.M., Steffen W.L. and Walker B.H. 1995. Terrestrial transects for global change research. Vegetatio 121: 53–65.

Larcher W. 1995. Physiological plant ecology: ecophysiology and stress physiology of functional groups. Springer-Verlag, Berlin; New York.

Medlyn B.E. 1998. Physiological basis of the light use efficiency model. Tree Physiology 18: 167–176.

Pearcy R.W. and Ehleringer.J. 1984. Comparative Ecophysiology of C3 and C4 plants. Plant, Cell and Environment 7: 1-13.

Porporato A., Laio F., Ridolfi L., Caylor K.K. and Rodriguez-Iturbe I. in review. Modeling the probability distribution function of soil moisture along the Kalahari Transect. Journal of Geophysical Research – Atmospheres.

Prince S.D. 1991. A model of regional primary production for use with coarse resolution satellite data. International Journal of Remote Sensing 12: 313-1330.

Privette J.L., Myneni R.B., Knyazikhin Y., Mukelabai M., Roberts G., Tian Y., Wang Y. and Leblanc S.G. 2002. Early spatial and temporal validation of MODIS LAI product in the southern Africa Kalahari. Remote Sensing of Environment. 83(12): 232–243.

Privette J.L., Tian Y., Roberts G., Scholes R.J., Wang Y., Caylor K.K., Frost P. and Mukelabai M. in press. Vegetation structure characteristics and relationships of Kalahari woodlands and savannas. Global Change Biology.

Rodriguez-Iturbe I., D'Odorico P., Porporato A. and Ridolfi. L. 1999. On the spatial and temporal links between vegetation, climate, and soil moisture. Water Resources Research 35: 3709–3722.

Scanlon T.M. and Albertson J.D. in press. Canopy scale measurements of CO2 and water vapor exchange along a precipitation gradient in southern Africa. Global Change Biology.

Scholes R.J., Dowty P.R., Caylor K., Parsons D.A.B., Frost P.G.H. and Shugart H.H. 2002. Trends in savanna structure and composition on an aridity gradient in the Kalahari. Journal of Vegetation Science 13: 419–428.

Scholes R.J. and Archer S.R. 1997. Tree-grass interactions in Savannas. Annual Review of Ecology and Systematics. 28: 517–544.

Scholes R.J. and Hall D.O. 1996. The Carbon Budget of Tropical Savannas, Woodlands and Grasslands, Pages 69-100. In: Breymeyer A.I., Hall D.O., Melillo J.M. and Agren G.I. (eds), Global Change: Effects on Coniferous Forests and Grasslands. John Wiley and Sons Ltd.

Scholes R.J., and Vanbreemen N. 1997. The Effects of Global Change On Tropical Ecosystems. Geoderma 79: 9–24.

Scholes R.J. and Walker B.H. 1993. An African Savanna: Synthesis of the Nylsvley Study. Cambridge University Press, Cambridge, UK.

Sellers P.J., Randall D.A., Collatz G.J., Berry J.A., Field C.B., Dazlich D.A., Zhang C., Collelo G.D. and Bounoua L. 1996. A Re-

vised Land Surface Parameterization (SiB2) for Atmospheric GCMs. Part I: Model Formulation. Journal of Climate 9: 676–705.

Shugart H.H. 1984. A Theory of Forest Dynamics. Springer-Verlag, New York, New York, USA.

Shugart H.H. 1998. Terrestrial Ecosystems in Changing Environments. Cambridge University Press, New York, New York, USA.

Skarpe C. 1991. Spatial patterns and dynamics of woody vegetation in an arid savanna. Journal of Vegetation Science 2: 565–572.

Smit G.N. and Rethman N.F.G. 2000. The influence of tree thinning on the soil water in a semi-arid savanna of southern Africa. Journal of Arid Environments 44: 41–59.

Smith T.M., and Goodman P.S. 1986. The effect of competition on the structure and dynamics of Acacia savannas in southern Africa. Journal of Ecology 74: 1031–1044.

Thomas D.S.G. and Shaw P.A. 1991. The Kalahari Environment. Cambridge University Press, Cambridge, UK.

Walker B.H. 1987. Determinants of tropical savannas. IRL Press, Oxford, UK.

Woodward F.I. and Smith T.M. 1994. Global photosynthesis and stomatal conductance: Modelling the controls by soils and climate. Advances in Botanical Research 20: 1–41.

Woodward F.I., Smith T.M. and Emanuel W.R. 1995. A global land primary productivity and phytogeography model. Global biogeochemical cycles 9: 471–490.